Electronic Supplementary Material (ESI) for Soft Matter.

Supporting Information for:

Understanding the drop impact onto moving hydrophilic and hydrophobic surfaces

H. Almohammadi and A. Amirfazli*

Department of Mechanical Engineering, York University, Toronto,

ON, M3J 1P3, Canada

*Corresponding Author

A. Amirfazli: +1-416-736-5901; Email: alidad2@yorku.ca

1. Spreading time (t_{max})

Drop spreading time (t_{max}) versus surface velocity on hydrophilic and hydrophobic surfaces is shown in Figures S1a and Figure S1b, respectively. Starting with a stationary surface (V_s=0), the results in Figure S1 show that the t_{max} is independent of We_n for hydrophobic surfaces; while it is affected by We_n for hydrophilic surfaces. In addition, it can be seen from Figure S1 that the t_{max} value decreases almost linearly as the surface velocity increases. The 'a' values in Figure S1 indicate the slope of the trend for t_{max} which is slightly lower for hydrophobic surfaces compared to that of hydrophilic surfaces.

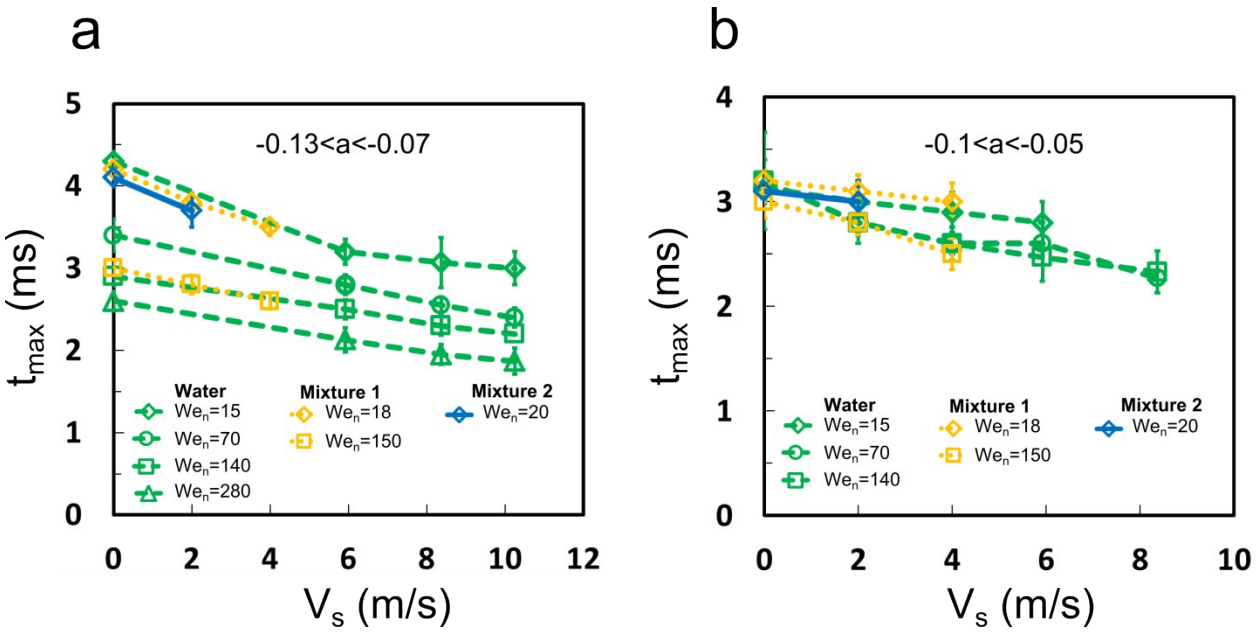

Figure S1. Experimental data for drop spreading time (t_{max}) versus surface velocity. Surfaces are (a) hydrophilic and (b) hydrophobic. *a* is the slope of linear function fitted to data. Color plot online.

2. Surfaces roughness details

Figure S2 shows the profiles of the surfaces used in this study. The values of the surface descriptors are provided in Table S1.

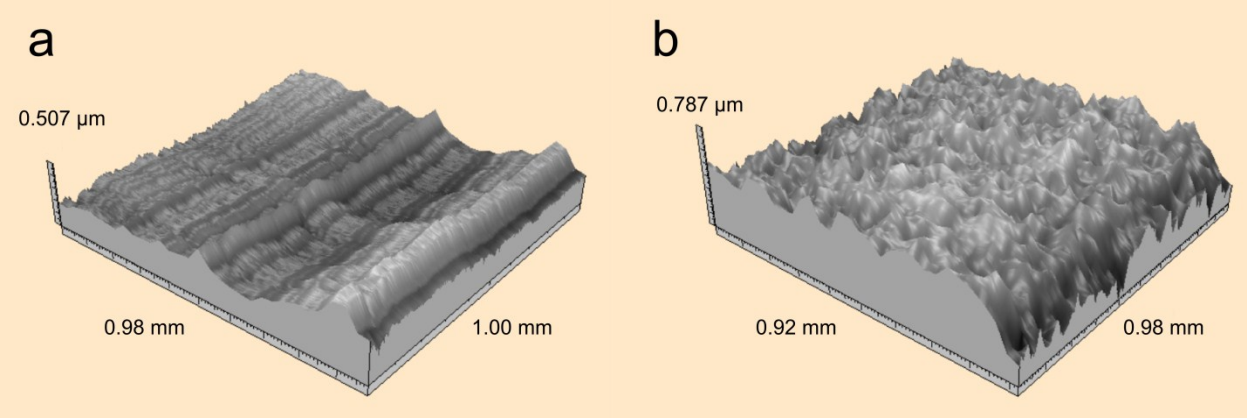

Figure S2. Surface profielometery of the (a) stainless steel, and (b) Teflon coated stainless steel.

Table S1. Surface descriptor values for stainless steel, and Teflon coated stainless steel.

Surface parameters	Stainless steel	Teflon coated stainless steel
Arithmetical mean height of the surface (Sa)	53±1 nm	88±15 nm
Root mean square height of the surface (Sq)	69±4 nm	112±20 nm
Maximum height of peaks (Sp)	232±45 nm	350±21 nm
Maximum height of valleys (Sv)	354±109 nm	556±102 nm
Skewness of height distribution (Ssk)	103±486	-527±287
Kurtosis of height distribution (Sku)	3736±753	3520±383

3. Moving surface

The assumption that the target surface is flat is justified in two ways:

First, the deviation of the surface in the frame of study is calculated using the following approach (see Figure S3):

$$Deviation\ \% = \frac{\delta}{X} \times 100 \qquad (S1)$$

where δ is the deviation of the surface from horizontal line in the frame of study (i.e. X, see Figure S3). To calculate the largest possible deviation, the X is considered to be the largest spreading diameter measured for the range of drop velocity tested in the current work. The X was measured to be 12.06 mm. The δ is calculated using following trigonometry calculation (see Figure S3):

$$R^2 = (R - \delta)^2 + (X/2)^2 \qquad (S2)$$

where R is the radius of the wheel ($R = 284.5\ mm$). Using equations S1 and S2, the deviation percentage is found to be 0.53%, which confirms that one can consider the target surface as flat.

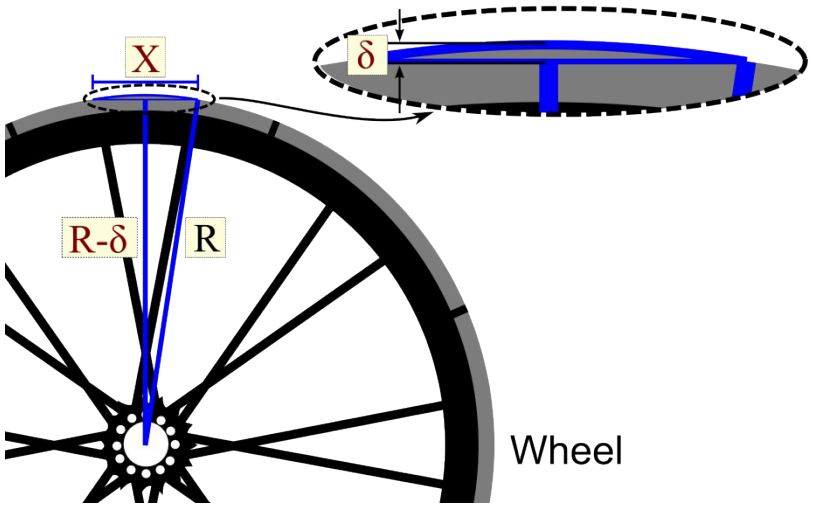

Figure S3. Schematic view of the wheel used in this study. Zoomed view in the inset shows the deviation of the surface from horizontal line in the frame of study.

The second approach to support the assumption that the target surface is flat is as follows. As it is apparent from the experimental setup configuration (see Figures 2 and S3), the surface has a curvature only in one direction, i.e. $r_1(t)$ direction in Figure S4; there is no curvature in the direction that is perpendicular to $r_1(t)$. The perpendicular direction to $r_1(t)$ is defined as $r_2(t)$ (see Figure S4). As such, for a given condition, the spreading radius of the drop on stationary condition are measured in both $r_1(t)$ and $r_2(t)$ directions (see Figure S4). The results for both hydrophilic and hydrophobic surfaces, and various drop velocities ranging from 0.5 to 3.4 m/s are shown in Figure S4. The results reveal that $r_1(t)$ is equal to $r_2(t)$ for all of the conditions; this means that the drop spreads symmetric over the surface same as that of perfectly flat surface in litertaure[6-8]. In other words, there is no curvature effect on drop spreading.

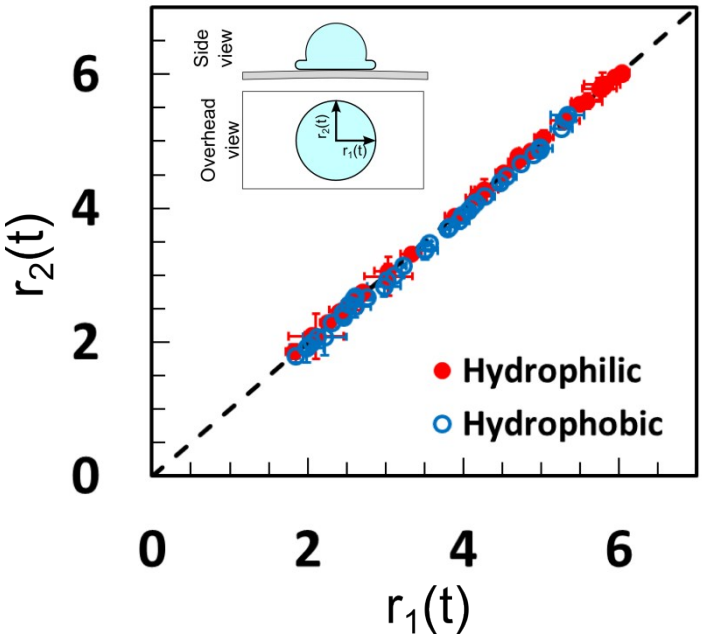

Figure S4. Comparison of spreading radius measured in two perpendicular directions, i.e. $r_1(t)$ and $r_2(t)$; where surface has curvature only in $r_1(t)$ direction. Dashed line refers to conditions where $r_1(t)$ is equal to $r_2(t)$.

4. Drop impact process

Figure S5 shows experimental results of a drop impacting onto moving hydrophilic and hydrophobic surfaces in the Eulerian frame of reference. To check the vertical movement of drop bulk, the highest surface velocity (V_s=17 m/s) and liquid viscosity (mixture 2) are considered as the extreme conditions; these conditions can have the highest possible momentum transfer from the surface to liquid. The results are provided for both highest (V_n= 3.4 m/s) and lowest drop (V_n=0.5 m/s) velocities considered in this study. As it is seen, the bulk of the drop moves only in vertical direction during impact process, which confirms that the vertical movement of drop bulk is true for all of the systems in this study.

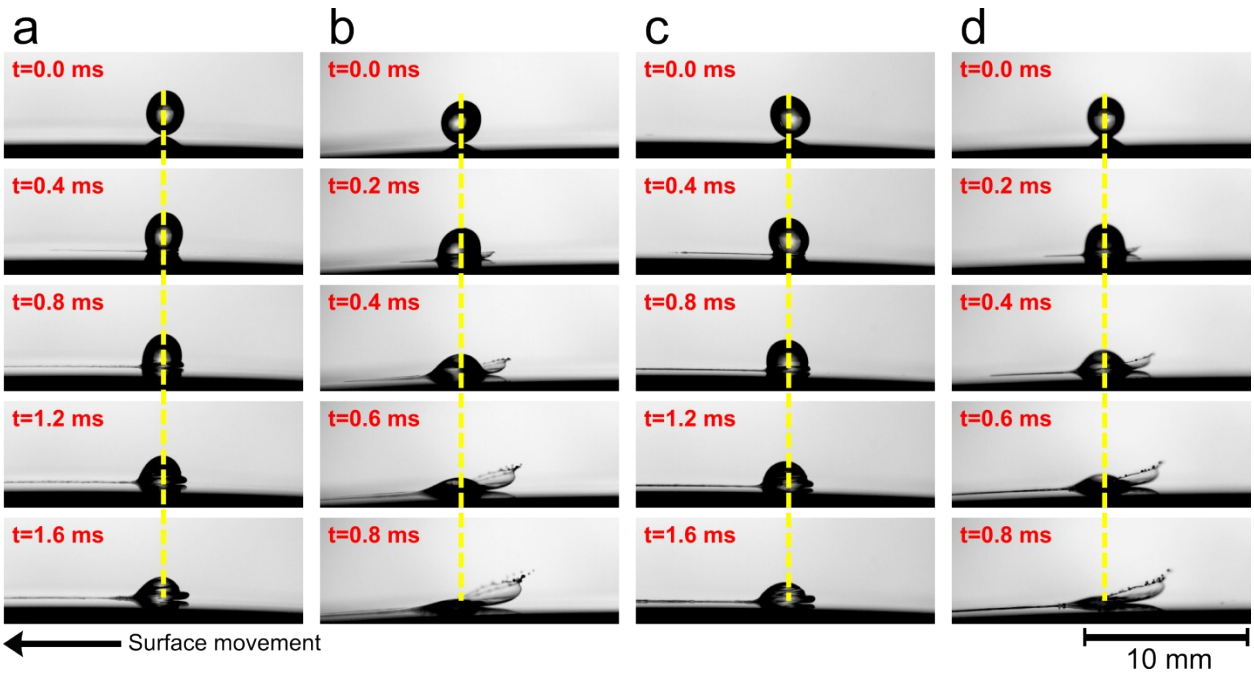

Figure S5. Side view of the drop impact on moving (a and b) hydrophilic, and (c and d) hydrophobic surfaces. Surface velocity is V_s= 17.0 m/s and drop (mixture 2) velocities are (a and c) V_n= 0.5 m/s, and (b and d) V_n= 3.4 m/s. Vertical dashed line shows the drop apex point; apex only moves in the vertical direction. Surface moves from right to left.

5. Modeling

Here we show that if one considers the following model which includes all of the non-dimensional numbers used in the literature to describe drop splashing, the end result can be simplified to Eq. 2 as provided in the main text. Considering the relative importance of the kinetic, viscous, and surface energies in splashing of a drop, one can write:

$$We_n{}^a Re_n{}^b Ca_n{}^c = K$$

Knowing that $Ca_n = We_n/Re_n$, one has:

$$We_n{}^a Re_n{}^b \frac{We_n{}^c}{Re_n{}^c} = K$$

where it can be written as:

$$We_n{}^{a+c} Re_n{}^{b-c} = K$$

Taking the root of both sides to the power of (a+c), one has:

$$We_n Re_n{}^{(b-c)/(a+c)} = K^{1/(a+c)}$$

Finally, by renaming the powers, one has:

$$We_n Re_n{}^{\alpha} = K_1$$

Considering above, it is clear that the Eq. 2 is a proper form to build a model for finding the threshold of splashing.

6. Curve fitting

The experimental results which are used to determine the values of the coefficients in Eq. 11 are shown in Figure S6 (symbols *). Each * symbol refers to a condition where the drop splashes azimuthally asymmetrically over the surface. The extent of the splashing (i.e. φ value) is different for each drop impact condition.

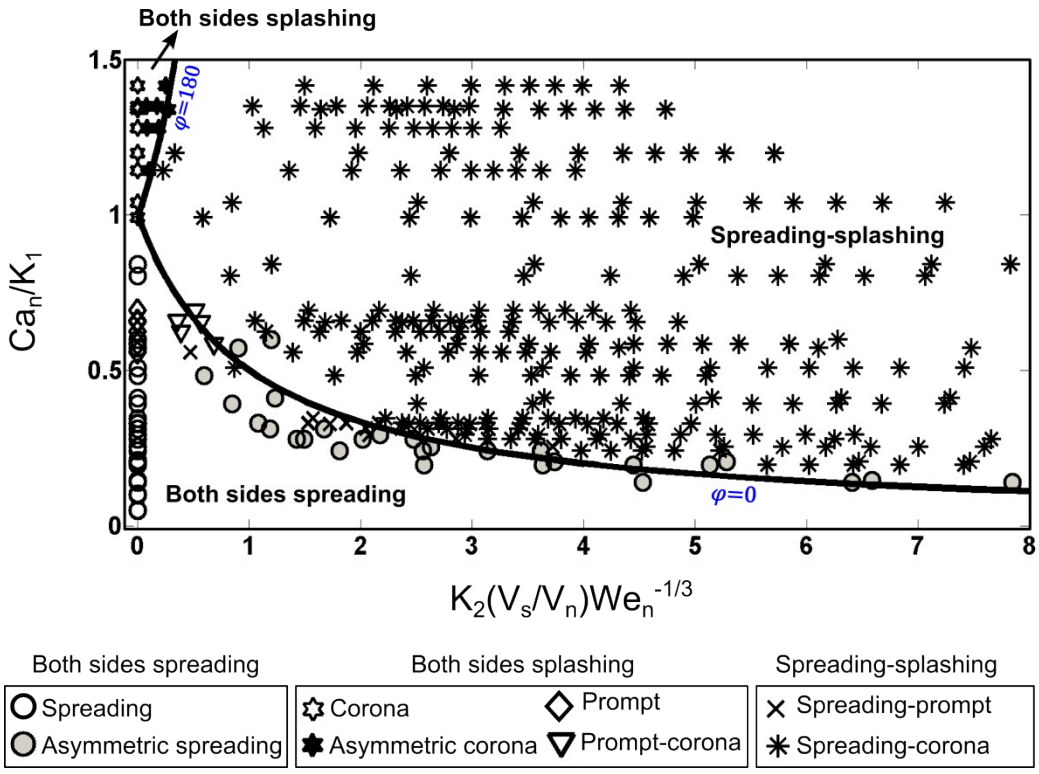

Figure S6. Experimental data of drop impact onto moving hydrophilic and hydrophobic surfaces (symbols). The model predication (Eq. 11) for $\varphi = 0°$ and $180°$ are shown with solid lines. The line delineate spreading and splashing zones for $\varphi = 0°$ and $180°$. Within the spreading-splashing regime, depending on drop impact condition, the splashing happens with different φ values.

Figure S7 presents the experimental data of φ versus the values predicted by the developed model (Eq. 11). Each symbol corresponds to certain drop impact condition. The value of φ corresponding to each drop impact condition is experimentally measured (x axis in Figure S7) and compared with the predication by Eq. 11 (y axis in Figure S7). Various drop impact conditions, i.e. different drop and surface velocities, liquid viscosities, and surface wettabilities, are considered in Figure S7. As it is shown, there is a good agreement between experimental data and the model prediction.

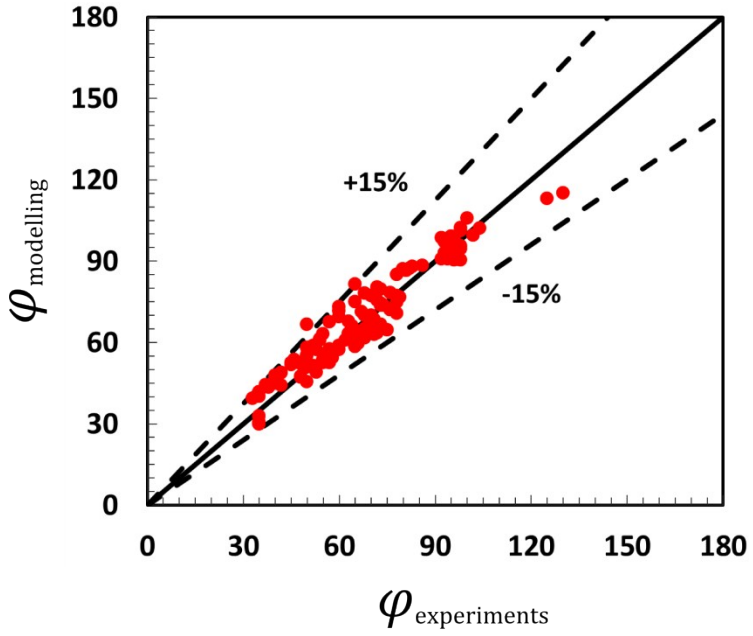

Figure S7. Comparison of the measured φ for drop splashing with the modelling prediction (i.e. Eq. 11). Solid line refers to conditions where experimental data are equal to model prediction (0% deviation).